

# First order Fermi acceleration at multiple oblique shocks

U.D.J. Gieseler and T.W. Jones

University of Minnesota, Department of Astronomy, 116 Church St. S.E., Minneapolis, MN 55455, USA

Received 14 October 1999 / 2 March 2000

**Abstract.** Numerical results for particle acceleration at multiple oblique shocks are presented. We calculate the steady state spectral slope of test particles accelerated by the first order Fermi process. The results are compared to analytical treatments for parameters where the diffusion approximation does apply. Effects of injection and finite shock extent are included phenomenologically. We find the spectrum of accelerated particles to harden substantially at multiple oblique shocks and discuss the influence of the number of shocks compared to the obliquity itself.

**Key words:** acceleration of particles – shock waves – methods: numerical – ISM: cosmic rays

## 1. Introduction

The theory of first order Fermi acceleration is commonly used to understand non thermal particle spectra or source distributions of synchrotron radiation in various astrophysical objects (for reviews see Drury 1983; Blandford & Eichler 1987; Kirk et al. 1994). In the diffusion approximation the steady-state spectral index of accelerated test particles is solely a function of the compression ratio of the shocked plasma flow. For strong shocks, the compression ratio is given by  $r = \rho'/\rho = 4$ , where  $\rho'$  and  $\rho$  are the downstream and upstream densities respectively. This leads to a phase space distribution of accelerated particles  $f(p) \propto p^{-s}$  with the canonical spectral index  $s = s_c := 3r/(r-1) = 4$ . The synchrotron emission of such an (e.g.) electron distribution as a function of frequency is given by  $\epsilon(\nu) \propto \nu^{-\alpha}$ , where  $\alpha = (s-3)/2$ . Unless the injection into the acceleration process is very effective, (leading to a strongly modified shock structure), this is the hardest spectrum which can be produced through first order Fermi acceleration by a single shock for which the diffusion approximation is valid. In complex large scale structures like the galaxy or active galactic nuclei (AGN) particles may encounter several shocks. If the transport time between shocks is larger than the acceleration time at a single shock, the problem can be described by subsequent shocks, where (in the case of planar geometry) the downstream distribution is transported (and decompressed) upstream of the next shock.

It is well known from the theory of diffusive shock acceleration, that the supply of an upstream power law distribution with the canonical spectral index leads to an amplification of the distribution, and the spectral index is not changed. However, the increased number of high energy particles is accompanied by a decrease of the number density at the low energy cutoff, leading to a flattening of the distribution at intermediate energies. This can be seen by calculating the spectrum as it is processed through a number of shocks, suppressing new injection, and considering adiabatic decompression, as shown by Melrose & Pope (1993). At sufficiently high energies, a power law with the canonical spectral index is always revealed. This applies for multiple identical shocks without losses, which are subject of this work.<sup>1</sup>

In the limit of an infinite number of subsequent shocks with injection at each shock, the flattening of the spectrum (compared to a single shock) extends even to the highest energy particles, with a momentum dependence of  $f(p) \propto p^{-3}$  (White 1985; Achterberg 1990).

Since the modification of the particle spectrum evolves from the low energy part of the spectrum due to further acceleration and adiabatic decompression, effects of injection can be very important. Including a theory of the injection process is well beyond the scope of this work. However, given a momentum  $p_0$  at which particles are injected, we assume, that this is the momentum that divides particles which are able to diffuse across the shock from the thermal pool. Adiabatic decompression can shift the momentum of some particles to  $p < p_0$ . These particles are considered to be ‘re-thermalised’ and no longer take part in the acceleration process and the resulting spectrum.

In order to compare our numerical work with analytical treatments we first consider subsequent identical shocks with a quasi-parallel magnetic field, leading to diffusive acceleration. The relative orientation of magnetic field and shock normal is, however, very likely to be oblique. Then, the diffusion approximation may no longer apply. To investigate the principal effect of a low number of multiple oblique shocks, we use for each shock the same inclination angle  $\Phi$  between magnetic field and shock normal in the upstream rest frame. We use a fixed escape probability  $P_{\text{esc}}$  for particles during the propagation between subsequent planar shocks to account for effects of

---

<sup>1</sup> For a consideration of synchrotron losses in the framework of multiple shocks, see e.g. Marcowith & Kirk (1999) and the references therein.

finite shock extension.<sup>2</sup> The acceleration process is described by the shock-drift mechanism. We take into account that multiple shock encounters are possible. For highly oblique geometry, repeated reflections off the compressed downstream field are the most important acceleration process. The transport upstream and downstream is of diffusive character, but the phase space distribution at the shock can be highly anisotropic, and the standard diffusion approximation of the acceleration problem (namely,  $f(x, p, \mu)$  is only to second order anisotropic) does not apply.

Even if we consider shocks with different inclination angles  $\Phi$ , each shock will produce locally a characteristic pitch-angle distribution, and spectral index. Only during the transport from one shock to the next, the pitch-angle distribution is isotropised. Anastasiadis & Vlahos (1993) used a random pitch angle before every electron shock interaction. This isotropisation produces steeper spectra as opposed to pitch-angle scattering, as shown by Naito & Takahara (1995).

After referring to some analytical results in Sect. 2, we compare our Monte-Carlo results for multiple identical planar shocks to analytical calculations in Sect. 3.1, where we also include effects of finite spatial extend of the shocks, and re-thermalisation. In Sect. 3.2 we present results for multiple oblique shocks.

## 2. Analytical considerations

In the diffusion approximation, the problem of subsequent shocks can be solved analytically. For an upstream phase-space distribution  $f_{u,1}(p, p_0)$ , the downstream distribution without additional injection is given by

$$f_{d,1}(p, p_0) = s_c p^{-s_c} \int_{p_0}^p dp' (p')^{s_c-1} f_{u,1}(p'). \quad (1)$$

During transport to the next shock, due to conservation of the phase space volume  $p^3/\rho$ , we have to consider the effect of the decompression of the plasma on the momentum of the particles. Expansion of the plasma by the compression ratio  $r$  leads to the shift of the downstream momentum  $p'$  to the new upstream momentum  $p = p'/r^{1/3}$  at the next shock (Schneider 1993). Applying Eq. (1) to  $N$  subsequent identical shocks with adiabatic decompression between them, we get the spectral index downstream of the  $N$ th shock for a delta-function injection distribution at  $p_0$  only at the first shock (see Melrose & Pope 1993):

$$s = \frac{3r}{r-1} - \frac{\log(e)}{\frac{\log(p/p_0)}{N-1} + \frac{1}{3} \ln(r) \log(e)} \equiv s_c - \Delta. \quad (2)$$

For exactly identical shocks, we have to consider injection at all shocks. The downstream distribution at the last shock is then given by a sum of the distributions injected with  $f(p, p_0) =$

$A \cdot \delta(p - p_0)$  at each shock:

$$f_{d,N}(p, p_0) = \sum_{n=0}^{N-1} \frac{A s_c^{n+1}}{n! p_0} \left( r^{\frac{n}{3}} \frac{p}{p_0} \right)^{-s_c} \left[ \ln \left( r^{\frac{n}{3}} \frac{p}{p_0} \right) \right]^n, \quad (3)$$

where the  $n$ th contribution is calculated by subsequent application of Eq. (1), and considering decompression between the shocks, as shown by Melrose & Pope (1993). The spectral index<sup>3</sup> is given by  $s = -\partial \ln[f_{d,N}(p, p_0)] / \partial \ln(p)$ , which can be easily calculated for  $N = 5$  shocks, which we consider here. For an infinite number of shocks, the result asymptotes to  $f_{d,\infty}(p, p_0) \propto p^{-3}$  (e.g., White 1985).

## 3. Monte-Carlo simulations

We present results for test-particle acceleration at multiple quasi-parallel and oblique shocks. We have used a Monte-Carlo code which was described by Gieseler et al. (1999), and extended it to multiple shocks. We refer to this previous work for a more detailed description of the code, and summarize here only the main features. A particle is described by three coordinates: the distance from the shock, the magnitude of the momentum  $p = |\mathbf{p}|$ , and the pitch angle  $\mu = \cos \alpha = \mathbf{p} \cdot \mathbf{B} / (pB)$  between particle momentum  $\mathbf{p}$  and magnetic field  $\mathbf{B}$ . Upstream and downstream the particle momentum is conserved, and the small scale irregularities lead to pitch-angle scattering. We do not consider cross field diffusion. The magnetic moment  $p(1 - \mu^2)/B$  is always conserved in the non-relativistic shocks with velocity  $u_s = 0.1c \equiv 0.1$ , which we consider here. When a particle crosses the shock, the momentum and pitch angle are transformed to the new relevant rest frame. Depending on the pitch angle  $\mu$  and inclination angle  $\Phi$ , particles can be reflected upstream of the shock. If a particle reaches a distance of a few diffusion length scales downstream of the shock where the density distribution has reached its constant downstream value, it is considered as escaped from the single shock. Between shocks, decompression of the plasma leads to a shift in the momentum distribution, as described in Sect. 2.

For exactly planar shocks, every escaping particle will reach the next shock, and can be further accelerated. To account approximately for the more realistic situation that some particles found in the downstream region of the  $N$ th shock have been accelerated only at  $n < N$  shocks, we use the fixed escape probability  $P_{\text{esc}}$ . This gives the fraction of particles of the downstream distribution of each shock that will not be further accelerated. These particles remain in the system but bypass the following shocks and therefore contribute directly to the downstream distribution of the  $N$ th shock. Exactly planar shocks would be described by  $P_{\text{esc}} = 0$ , whereas  $P_{\text{esc}} = 1$  reveals a spectrum produced by one single shock.

The distinction of particles which are able to diffuse (and for which the shock is a discontinuity) from the thermal particles, which are not subject to the first order acceleration process, is based on the gyro radius, and therefore on the momentum of the

<sup>2</sup> The probability  $P_{\text{esc}}$ , which we introduced here, should not be confused with the escape probability for each shock acceleration cycle.

<sup>3</sup> We call the locally defined slope of the spectrum always spectral index, even where it is not a pure power law.

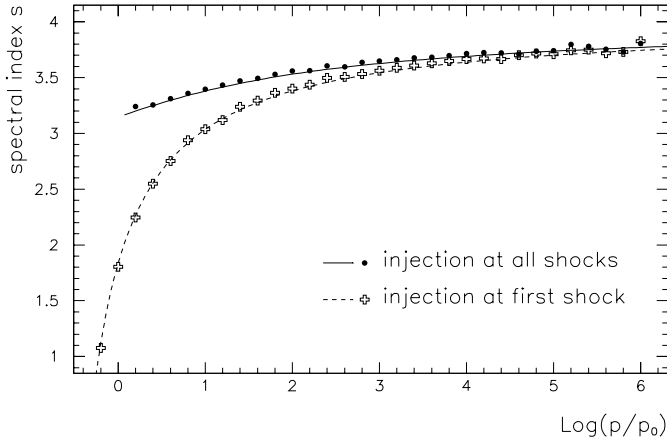


**Fig. 1.** Spectral index  $s$  vs. momentum  $p$ , downstream of 5th quasi-parallel shock. Discrete symbols show the Monte-Carlo results, whereas the lines represent analytical calculations. Parameters for all shocks are  $r = 4$ ,  $u_s = 0.1$ ,  $\Phi = 8.07$ ,  $u_s/\cos\Phi = 0.101$ .  $P_{\text{esc}} = 0$  and no re-thermalisation is used.

particles. We do not include a self consistent injection model here. Instead we inject particles with a momentum  $p_0/m = \gamma v = 10$ , for which they have an already relativistic velocity, and can be accelerated immediately. However, when a particle has a momentum  $p < p_0$ , we consider this particle as re-thermalised and suppress further acceleration, even though the momentum  $p_0$  does not correspond to a mean thermal momentum.

### 3.1. Multiple shocks with diffusive acceleration

In order to compare our Monte-Carlo simulations with analytical calculations, we first consider identical planar quasi-parallel shocks. Here, *all* particles are transported through the subsequent shocks with decompression between them. This corresponds to  $P_{\text{esc}} = 0$  for the escape probability. We also do not include effects of re-thermalisation. Therefore we can compare the results of the Monte-Carlo simulations directly to the analytical results described in Sect. 2. To retrieve the spectral index from the momentum distribution, we use the linear interpolation between two neighboring momentum bins in the region  $\log(p/p_0) < 3$ . The statistical fluctuation is then expressed solely by the scatter of the result in this region. For higher momenta, where the distribution deviates only slightly from a pure power law, we fit a power law over four equidistant momentum bins in  $\log(p)$ . The result for  $7.3 \cdot 10^5$  particles is presented in Fig. 1. The open crosses represent particles which are injected at the first shock with  $p = p_0$ . The final distribution is measured downstream of the 5th shock before decompression. Eq. (2) is shown by the dashed line. The filled dots show the spectral slope in the case when particles are injected at all shocks. The corresponding analytical result from a derivation of Eq. (3) is shown by the solid line in Fig. 1. In both cases, the agreement is quite good.

In Fig. 2 we have included effects of finite extent of the acceleration region by choosing the free parameter  $P_{\text{esc}} = 0.2$ , as described above. This leads essentially to a reduction of the

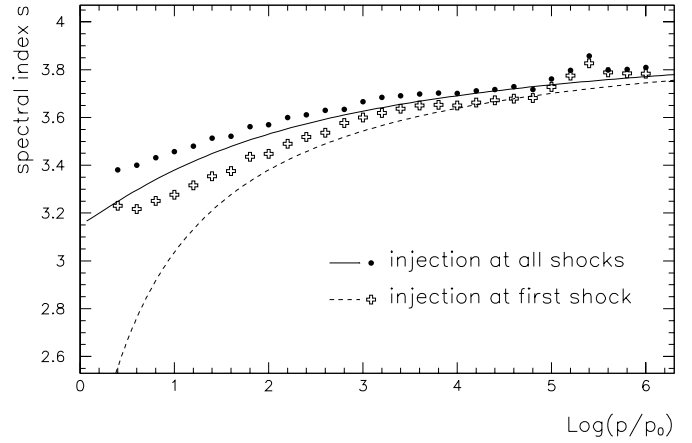


**Fig. 2.** Discrete symbols show the Monte-Carlo results for the spectral index  $s$  vs. momentum  $p$ , downstream of 5th quasi-parallel shock, including effects of escape with  $P_{\text{esc}} = 0.2$  and re-thermalisation. Shock parameters are the same as in Fig. 1. The lines are identical with those in Fig. 1 and are included here for comparison.

number of shocks at which the particles in the final downstream distribution have been accelerated, and therefore the momentum distribution is steeper. In addition we remove particles from the acceleration mechanism with momentum  $p < p_0$ , which correspond to re-thermalisation. This produces a cutoff of the test-particle distribution at  $\log(p/p_0) = 0$ . To show the effect of the escape, we have included in Fig. 2 the analytical results shown in Fig. 1 as lines. The discrete symbols represent the Monte-Carlo results. The number of initial particles here is  $2.1 \cdot 10^6$ . The symbols and the fit procedure used are the same as described above. Note that the distribution of particles injected at the first shock is a subset of the particles injected at all shocks. We do not perform independent runs of the code to measure these two momentum distributions. With increasing momentum, the distribution of particles injected at all shocks has an increasing fraction of particles which were injected at the first shock, because these have the highest probability to gain momentum. Therefore, the statistical fluctuations of the Monte-Carlo distributions shown in Fig. 2 (and also in Fig. 1 and Fig. 3) are correlated at high momentum.

### 3.2. Multiple oblique shocks

By increasing the inclination angle  $\Phi$ , the ratio of the particle velocity to the intersection velocity of magnetic field and shock becomes larger, and the acceleration can no longer be described by the diffusion approximation. Then, the calculations of Sect. 2 break down.

We consider here strong shocks with speed  $u_s = 0.1$ , and  $\Phi = 70.53$ . The resulting velocity of the intersection point is  $u_s/\cos\Phi = 0.3$ . Such a shock produces a spectrum with canonical index  $s_c = 3.45$  (Kirk & Heavens 1989). The realisation of the multiplicity we investigate here is one in which the compression by the shock and the decompression of the plasma described in Sect. 2 are both effective only along the shock nor-

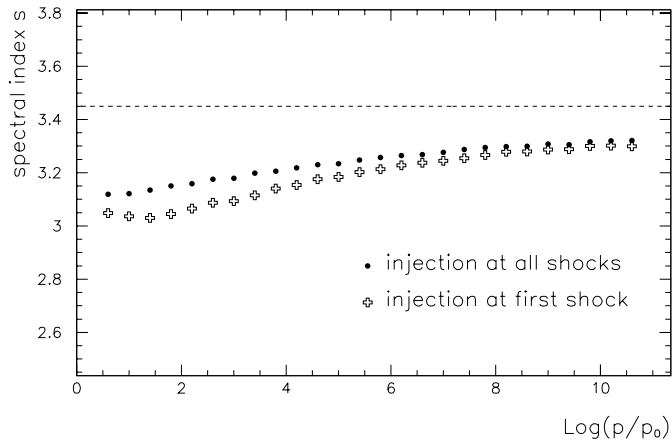


**Fig. 3.** Discrete symbols show the Monte-Carlo results for the spectral index  $s$  vs. momentum  $p$ , downstream of 5th oblique shock. The dashed line indicates the canonical spectral index  $s_c = 3.45$ . Parameters for all shocks are  $r = 4$ ,  $u_s = 0.1$ ,  $\Phi = 70.53$ ,  $u_s/\cos\Phi = 0.3$ . With escape  $P_{\text{esc}} = 0.2$  and re-thermalisation included.

mal (which has the same direction for all subsequent shocks). Therefore, the decompression will restore the magnetic field to the initial upstream value and orientation. This realisation can be described by multiple *identical* oblique shocks of the same inclination angle  $\Phi$ . This situation reveals most clearly the direct effect of the shock multiplicity, together with re-thermalisation and escape (for which we chose  $P_{\text{esc}} = 0.2$ ). The results are presented in Fig. 3, where the discrete symbols represent the Monte-Carlo calculations in the same way as described above, except that the linear interpolation of two adjacent bins is used up to  $\log(p/p_0) = 5$ , and an initial number of  $5.4 \cdot 10^6$  independent particles is simulated. The dashed line indicates the canonical spectral index  $s_c$  for a single shock of this type. Although the escape between shocks leads to a steepening of the spectrum towards the canonical result, the slope at multiple oblique shocks is still flatter than for a single shock. The *relative hardening*  $\Delta/s_c \equiv (s_c - s)/s_c$  due to the multiplicity of the shock is in the high energy part (from about three orders of magnitude above the injection momentum) quite similar to the diffusive case, shown in Fig. 2. However, the main effect of producing a hard spectrum is due to the obliquity ( $s_c = 3.45$  compared to  $s_c = 4$ ), and this is independent of momentum for relativistic particle velocities, as long no loss mechanisms are included.

#### 4. Conclusion

Our Monte-Carlo simulation of first order Fermi acceleration, using the shock-drift process and diffusively (or statistically) particle transport reproduced the analytical steady state test-particle spectrum at multiple shocks, for which the diffusion approximation does apply. We introduced a phenomenological re-thermalisation effect, which accounts for the fact, that below the injection momentum no acceleration can occur. Furthermore, with regard to the finite extension of the shock, we allowed for escape of particles between subsequent shocks. This

reduces the ability of multiple shocks to flatten the spectrum which would be produced at one single shock.

As a more realistic setup of multiple shock acceleration at fast shocks we considered oblique shocks, and included a finite escape probability  $P_{\text{esc}} = 0.2$  between shocks. We found very hard spectral distributions at strong shocks ( $r = 4$ ) with velocity  $u_s = 0.1$  and obliquity  $\Phi \simeq 70$ . The main effect here is produced by the obliquity, because the canonical spectral index is  $s_c = 3.45$ . In addition, the spectrum becomes even harder with  $s = 3.21 \pm 0.01$  at  $\log(p/p_0) = 4$  at the relatively low number  $N = 5$  of these moderately oblique shocks considered here (Fig. 3).

An example geometrical situation where multiple oblique shocks with (about) the same inclination angle  $\Phi$  are likely is a jet with helical magnetic field and along which a number of shocks exist. We assume, that the shocks are propagating along the jet axis and do not modify the jet geometry. The compression by the shock and the decompression of the plasma described in Sect. 2 are then both effective only along the shock normal. Therefore, the decompression will restore the initial upstream magnetic field orientation. This situation can be described by multiple *identical* oblique shocks. If the magnetic field would not be restored to the upstream direction, the obliquity for subsequent plan-parallel shocks would increase, leading to even harder spectra than described above.

In regions where geometrically uncorrelated shocks exist, like central regions of AGN, a *large* number of *subsequent* shocks, through which a single distribution is processed, might be a too strong idealisation. Here, we would have to average over a low number of shocks with different inclination angles  $\Phi$ . If we consider electrons, in addition effects of losses and magnetic field strength would generally have to be included. However, our results indicate, that very flat synchrotron spectra with index  $0 < \alpha = (s - 3)/2 < 0.5$  can be produced even at a low number ( $N < 10$ ) of oblique shocks.

*Acknowledgements.* U.G. acknowledges useful discussions with John Kirk. We thank the referee for helpful comments on the manuscript. This work was supported by the University of Minnesota Supercomputing Institute, by NSF grant AST-9619438 and by NASA grant NAG5-5055.

#### References

- Achterberg A., 1990, A&A 231, 251
- Anastasiadis A., Vlahos L., 1993, A&A 275, 427
- Blandford R.D., Eichler D., 1987, Physics Reports 154, 1
- Drury L. O'C., 1983, Rep. Prog. Phys. 46, 973
- Gieseler U.D.J., Kirk J.G., Gallant Y.A., Achterberg A., 1999, A&A 345, 298
- Kirk J.G., Heavens A.F., 1989, MNRAS 239, 995
- Kirk J.G., Melrose D.B., Priest E.R., 1994, In: Benz A.O., Courvoisier T.J.-L. (eds.) Plasma Astrophysics. Saas-Fee Advanced Course 24, Springer-Verlag, Berlin
- Marcowith A., Kirk J.G., 1999, A&A 347, 391
- Melrose D.B., Pope M.H., 1993, Proc. Astron. Soc. Aust. 10, 222
- Naito T., Takahara F., 1995, MNRAS 275, 1077
- Schneider P., 1993, A&A 278, 315
- White R.L., 1985, ApJ 289, 698